

# Width of phonon states on defects of various dimensions

L. A. Falkovsky <sup>\*</sup>

*Landau Institute for Theoretical Physics, 117337 Moscow, Russia*

## Abstract

We consider the localized phonon states created by defects of various geometries near the edge of an optical-phonon branch. The averaged Green's function is calculated to study the Raman line shape. The phonon scattering by the defects induces broadening and line shape asymmetry. The contribution of localized states to Raman spectra has a form of shoulder with a width proportional to the square root of defect concentration.

PACS: 63.20.-e, 78.30.-j

## I. INTRODUCTION

The interaction of elementary excitations with defects is an old problem of solid state physics. For the case of optical phonons, it has attracted considerable attention in recent years because of the Raman scattering applications for determination of the isotopic composition [1], for detection of stacking faults in polytypes [2,3], for investigations of residual strain and strain relaxation at interfaces in semiconductors [4].

A refinement of these effects takes the interactions among phonons and with defects into account.

(i) *The phonon decay* into two (or more) acoustic or optical phonons is possible even at zero temperature. These unharmonic processes give rise to the so-called natural width  $\Gamma^{\text{nat}} \sim \omega_0 \sqrt{m/M}$ , where  $\omega_0$  is the optical-phonon frequency,  $m$  and  $M$  are the electron and atom masses. In spite of the small value  $\sqrt{m/M} \sim 10^{-2}$ , the decay processes give the observable linewidth in Raman spectra and the quite small mean-free path  $r_\gamma \sim a \sqrt{\omega_0 / \Gamma^{\text{nat}}} \sim 10a$ , where  $a$  is the lattice constant. The decay cross section depends weakly on the phonon frequency since no singularities exist in the final density of states for that processes. Therefore, the natural optical-phonon width  $\Gamma^{\text{nat}}$  can be considered for given material as constant up to room temperatures and for the phonon frequency varying in a small interval of the order of  $\Gamma^{\text{nat}}$ . Then we obtain for perfect crystals the Lorentzian line shape of Raman spectra.

(ii) *The phonon interaction with defects* should be considered in two aspects. First, it gives rise to elastic phonon scattering and makes an additional contribution to the phonon width  $\Gamma$ . This contribution (linear in defect concentration  $c$ ) can be evaluated [5] using

---

<sup>\*</sup>e-mail: falk@itp.ac.ru

the golden rule of quantum mechanics. The scattering by defects, being elastic, conserves singularities of the phonon density of states. This is important for the Raman scattering, because we are interested in phonons with small wave vectors. For the short-range potential of defects with the radius of the order of  $a < r_\gamma$ , the singularity arises also in the width  $\Gamma$  as function of phonon frequency  $\omega$  at the phonon branch edge, i.e., at the maximum (or minimum) value  $\omega_0$ . Thus we obtain the asymmetrical Raman line shape, that was observed in experiments with 3C-SiC [4]. This asymmetry is sensitive to the defect geometry, which may have the point, line or plain form [6]. Secondly, the interaction with defects can result in appearance of new modes. For instance, the mode forbidden by selection rules in perfect crystals at given experimental conditions has been observed in crystals with the stacking faults which give an example of plain defects in SiC polytypes [2]. Some additional modes were found also in computer simulations for the sequence of number layers with the stacking faults [3]. In addition, the localized mode can be associated with defects [7].

The problem of localized states on the single isotopic defect has the exact solution. However, the case of the low, but finite defect concentration involves serious difficulties [8,9]. That is because the solution should be self-consistent for the large distances essential near the edge of phonon branches. If the natural width is ignored, the answer obtained in the series expansion of the phonon self-energy is the following. The edge of phonon branches is displaced linearly in  $c$  and the band of localized states arises with a width of the order of  $c^2$ . This  $c^2$  behavior is explained by fluctuations in the spatial distribution of defects.

The aim of the present paper is to consider (taking the natural width into account) the situation when the states localized on defects can exist. We are especially interested in the case when the localized states appear near an edge of optical-phonon branches. Broadening of localized states is found just in the lowest order in the defect concentration  $c$ , if this additional width is larger than the natural phonon width. This unusual behavior is conditioned by the resonance interaction of localized states with the close edge of the extended phonon branch. The defects of different geometries are treated such as point defects, line defects involved by dislocations, and plain defects produced by stacking faults or by the crystallite boundaries. They give the different broadening and asymmetry of the Raman line shape. The preliminary results of the work were published in Ref. [10].

## II. INTERACTION OF PHONON MODES WITH DEFECTS

We solve the equation for the phonon Green's function in the form:

$$D(\mathbf{r}, \mathbf{r}', \omega) = D_0(\mathbf{r} - \mathbf{r}', \omega) - \int d\mathbf{r}'' D_0(\mathbf{r} - \mathbf{r}'', \omega) U(\mathbf{r}'') D(\mathbf{r}'', \mathbf{r}', \omega), \quad (1)$$

where the interaction with defects located in points  $\mathbf{r}_n$  is

$$U(\mathbf{r}) = \sum_n u(\mathbf{r} - \mathbf{r}_n) = \sum_{\mathbf{n}, \mathbf{q}} u(\mathbf{q}) e^{i\mathbf{q}(\mathbf{r} - \mathbf{r}_n)}.$$

For an isotopic defect,  $u(\mathbf{q})$  is constant:  $u(\mathbf{q}) = u_0 = (M_0 - M)a^3/M_0$ , where  $M$  and  $M_0$  are the masses of the defect atom and the host atom, respectively,  $a$  is the lattice constant. In the following, the large distances from the defect on the atomic scale are important. Then

for any type of defects, we can set the Fourier component  $u(\mathbf{q})$  equal to the constant  $u_0$  supposing the short-range potential. For the same reason we expand the phonon spectrum near the Brillouin-zone center taking the Green's function in the absence of defects as

$$D_0(k, \omega) = (\omega_0^2 - s^2 k^2 - \omega^2 - i\omega\Gamma^{\text{nat}})^{-1},$$

where the natural phonon width  $\Gamma^{\text{nat}}$  is connected to decay into acoustic or optical phonons.

The imaginary part of  $D(\mathbf{k}, \omega)$  gives the differential density of squared frequencies. In addition, the Raman intensity  $I(\omega)$  for phonon excitation with frequency  $\omega$  and momentum  $\mathbf{k}$  is proportional to  $\text{Im}D(\mathbf{k}, \omega)$  which gives the Lorentzian line shape in the absence of defects

$$I(\omega) \sim \text{Im}D_0(\mathbf{k}, \omega) = \frac{\omega\Gamma^{\text{nat}}}{(\omega_0^2 - s^2 k^2 - \omega^2)^2 + (\omega\Gamma^{\text{nat}})^2},$$

if  $\Gamma^{\text{nat}}$  is assumed to be small in comparison to the frequency  $\omega_0$ .

In the presence of defects, the Green's function must be averaged over defect positions. It is convenient to use the well-known diagram technique for impurities scattering [11]. This method can be modified [12] in order to take the possible localized states into account. Performing the iterations of Eq. (1) in  $U(\mathbf{r})$  and averaging over the defect positions, we have for the sum of noncrossing diagrams:

$$\begin{aligned} D(\mathbf{k}, \omega) &= D_0(k, \omega) + cD_0^2(k, \omega) \\ &\times \sum_{n=0}^{\infty} (-u_0)^{n+1} \left( cD_0(k, \omega) + \sum_q D(\mathbf{q}, \omega) \right)^n, \end{aligned} \quad (2)$$

which gives after some algebra

$$D(\mathbf{k}, \omega)^{-1} = D_0(k, \omega)^{-1} + cu_0 \left( 1 + u_0 \sum_q D(\mathbf{q}, \omega) \right)^{-1}. \quad (3)$$

The term of first order only in the defect concentration  $c$  is held in the phonon self-energy given by the second term on the right-hand side of Eq. (3), since we assume that the distance between defects ( $r_c \propto c^{-1/2}$  for line defects) is larger, than the phonon mean-free path  $r_\gamma$ .

Let us emphasize that the phonon self-energy involves the perturbed function  $D(\mathbf{q}, \omega)$ , but not  $D_0(\mathbf{q}, \omega)$ . Then the Green's function  $D(\mathbf{q}, \omega)$  has to be found from the integral equation (3). Integration (summation) is performed with respect to the 3D-vector  $\mathbf{q}$  for point defects, over the 2D-vector  $\mathbf{q}_\perp$  for line defects (then  $q_z = k_z$ ), and over  $q_z$  for plain defects (then  $\mathbf{q}_\parallel = \mathbf{k}_\parallel$ ).

The integral equation (3) can be reduced to an algebraic equation. We introduce the new unknown function  $\zeta$  and the complex variable  $\zeta_0$  in the case of point defects by the definition

$$D(\mathbf{k}, \omega) = (\zeta - s^2 k^2)^{-1}, \quad \zeta_0 = \omega_0^2 - \omega^2 - i\omega\Gamma^{\text{nat}}.$$

Then Eq. (3) gives

$$\zeta = \zeta_0 + c\omega_0^3 \left( \frac{\kappa}{\lambda} - \kappa + \frac{\pi}{2} \sqrt{-\zeta} \right)^{-1}. \quad (4)$$

In the case of line defects

$$D(\mathbf{k}, \omega) = (\zeta - s^2 k_{\perp}^2)^{-1}, \quad \zeta_0 = \omega_0^2 - s^2 k_z^2 - \omega^2 - i\omega\Gamma^{\text{nat}}$$

and we obtain

$$\zeta = \zeta_0 + c\omega_0^2 \left( \frac{1}{\lambda} - \ln \frac{\kappa^2}{-\zeta} \right)^{-1}. \quad (5)$$

For plain defects

$$D(\mathbf{k}, \omega) = (\zeta - s^2 k_z^2)^{-1}, \quad \zeta_0 = \omega_0^2 - s^2 k_{\parallel}^2 - \omega^2 - i\omega\Gamma^{\text{nat}},$$

we have

$$\zeta = \zeta_0 + c\omega_0^2 \left( \frac{1}{\lambda} - \frac{\omega_0}{\sqrt{-\zeta}} \right)^{-1}, \quad (6)$$

where  $\lambda$  is the dimensionless coupling constant proportional to  $u_0$ ,  $c$  is the atomic concentration of defects in 3D, 2D, or 1D region, respectively for the point, line, or plain defects,  $\kappa$  is the cutoff frequency, the  $z$  axis is taken in direction of the line defect or normal to the plane defect,  $\mathbf{k}_{\parallel}$  is parallel to the plane defect. The branches of  $\sqrt{-\zeta}$  and  $\ln(-\zeta)$  have to be taken in the upper half-plane. We consider the retarded Green's function which has no singularities in the upper half-plane of complex variable  $\omega$ .

The equations (4)–(6) have two singularities. One at  $\zeta = 0$  is related to the branch edge of the extended optical-phonon mode. Other at  $\zeta_l$  is related to the localized mode and determined by the zero of expressions in parentheses of Eqs. (4)–(6). For instance, for line defects we have

$$\frac{1}{\lambda} - \ln \frac{\kappa^2}{-\zeta_l} = 0$$

which gives

$$\zeta_l = -\kappa^2 e^{-1/\lambda}.$$

Notice, that the zero  $\zeta_l$  of the expressions in parentheses, if it exists, is negative. The zero can exist, if  $\lambda > 1$  in the case of point defects, and for any positive  $\lambda$  in the cases of both line and plain defects.

The situation is schematically explained in Fig. 1, where  $\zeta_0$  determined by Eqs. (4)–(6) is shown as function of  $\zeta$ . In the regions plotted by solid lines and indicated by the arrows 1, the solution  $\zeta$  is real for real values of  $\zeta_0$  and has no singularities in the upper half-plane of  $\omega$ , as it must be for the retarded Green's function. If  $\Gamma^{\text{nat}} = 0$ , this region makes no contribution to the density of phonon states. The second solution  $\zeta$  (dashed lines indicated by the arrows 2) corresponding to the same  $\zeta_0$  should be rejected since it has singularities in the upper half-plane. For real  $\zeta_0$ , the solution  $\zeta$  has the imaginary part in the regions shown by dot-dashed lines and indicated by arrows 3 and 4. The region 3 represents the extended phonon mode. The region 4 shows the localized states.

a) *Low concentration of defects: unrenormalized approximation.*

We can solve Eqs. (4)–(6) analytically supposing  $c$  to be small. Using the iterative method (if  $|\zeta - \zeta_0| \ll |\zeta_0|$ ) we obtain on the first step for point defects

$$\zeta = \zeta_0 + c\omega_0^3 \left( \frac{\kappa}{\lambda} - \kappa + \frac{\pi}{2} \sqrt{-\zeta_0} \right)^{-1}, \quad (7)$$

for line defects

$$\zeta = \zeta_0 + c\omega_0^2 \left( \frac{1}{\lambda} - \ln \frac{\kappa^2}{-\zeta_0} \right)^{-1}, \quad (8)$$

and for plain defects

$$\zeta = \zeta_0 + c\omega_0^2 \left( \frac{1}{\lambda} - \frac{\omega_0}{\sqrt{-\zeta_0}} \right)^{-1}. \quad (9)$$

This unrenormalized approach corresponds to substituting  $D_0(\mathbf{q}, \omega)$  for  $D(\mathbf{q}, \omega)$  in the self-energy of Eq. (3).

In Eqs. (7)–(9), the terms proportional to the concentration  $c$  represent the contribution of defects. If  $\text{Re } \zeta_0 > 0$ , i.e., for the region shown by the arrow 3 in Fig. 1, the frequency belongs to the extended states. Then the imaginary and real parts of the second terms on the right-hand side of Eqs. (7)–(9) give the phonon shift and the additional width induced by the defect - phonon scattering. If  $\text{Re } \zeta_0 < 0$  and for positive  $\lambda$ , the localized states can exist. In the absence of the natural width, they always exist for the cases both the line and plain defects, in accord with the well-known statement of quantum mechanics about the bound state in a shallow potential. However, for the finite value of  $\Gamma^{\text{nat}}$ , the coupling constant should be strong to give the substantial gap:  $\omega_l - \omega_0 \gg \Gamma^{\text{nat}}$ . This condition can be rewritten as  $r_l \ll r_\gamma$ , if we introduce the radius of localized states  $r_l = a\sqrt{\omega_0/(\omega_l - \omega_0)}$  and the phonon mean-free path  $r_\gamma = a\sqrt{\omega_0/\Gamma^{\text{nat}}}$ .

b) *Self-consistent approach: the square-root behavior.*

The conditions of validity for Eqs. (7)–(9) impose a constraint on the concentration of defects  $c$ . It is hard to satisfy the conditions of validity, if  $\zeta_0 \rightarrow \zeta_l$ . In fact, the equation  $\zeta_0 = \zeta_l$  determines the frequency  $\omega_l$  of localized phonon states. For  $|\zeta_0 - \zeta_l| \ll |\zeta_l|$ , we expand the expressions in parentheses of Eqs. (4)–(6) in  $(\zeta - \zeta_l)$  and arrive to the quadratic algebraic equation which has the solution

$$\zeta = \frac{\zeta_0 + \zeta_l}{2} + \sqrt{\frac{(\zeta_0 - \zeta_l)^2}{4} - bc}, \quad (10)$$

where  $b = 4(-\zeta_l)^{1/2}\omega_0^3/\pi$  for point defects,  $b = -\zeta_l\omega_0^2$  for line defects, and  $b = 2\omega_0(-\zeta_l)^{3/2}$  for plain defects. We notice again that the solution with the positive imaginary part should be taken in Eq. (10).

If  $\zeta_0 \rightarrow \zeta_l$ , we obtain a negative value under the square root in Eq. (10), that gives the imaginary part of  $\zeta$ . Then the imaginary part is determined in competition of  $\omega_0\Gamma^{\text{nat}}$  with  $2(bc)^{1/2}$ . The region where  $\Gamma^{\text{nat}} < 2(bc)^{1/2}/\omega_0$  is indicated by the arrow 4 in Fig. 1. This condition may be compatible with the conditions (i)  $r_c \gg r_\gamma$  for the expansion in terms of  $c$  used in Eq. (3) and (ii)  $r_\gamma \gg r_l$  for the existence of localized states. Here, the localized states make the maximal contribution to the differential density of states and to the Raman intensity,

$$\text{Im} \frac{1}{\zeta} = \frac{\sqrt{bc}}{\zeta^2}, \quad (11)$$

which is proportional to the square root of the defect concentration. In the opposite limit  $\Gamma^{\text{nat}} > 2(bc)^{1/2}/\omega_0$ , we can use the Eqs. (7)–(9) which give the contribution linear in the defect concentration.

c) *Self-consistent approach: the numerical solution.*

As a matter of fact, each of the equations (4), (5), and (6) is a system of two equations for the real and imaginary parts of  $\zeta$ . This system may be solved numerically. It is convenient to introduce the unknown real variables  $x$  and  $y$  as

$$-\zeta = \sqrt{x^2 + y^2} \exp \left[ i \left( \frac{\pi}{2} - \arctan \frac{x}{y} \right) \right]$$

supposing  $y > 0$  and  $-\pi/2 < \arctan z < \pi/2$  in order to comply with the analytical requirements in the upper-half plain. The similar form is used also for  $\zeta_0$  with  $x \rightarrow \omega^2 - \omega_0^2$  and  $y \rightarrow \omega \Gamma^{\text{nat}}$ .

The results of the numerical solution are shown by solid lines in Fig. 2 (line defects) and in Fig. 3 (plain defects) for the cases, when the coupling constant  $\lambda$  is negative and no localized states exist. We used the values of  $\omega_0 = 520 \text{ cm}^{-1}$  and  $\Gamma^{\text{nat}} = 3.2 \text{ cm}^{-1}$ , which correspond to pure silicon, and the cutoff parameter  $\kappa = \omega_0$ . The unrenormalized approximation is shown by dashed lines. We see that the interaction of phonons with defects results in broadening and shift of the Raman line from the position (dotted line) in the absence of defects.

The broadening is much more on the low-frequency side of the line than on the high-frequency side, that gives the line shape asymmetry. This is an effect of the phonon density of states: the elastic interaction with defects makes a contribution to the phonon life-time only in the region  $\omega^2 < \omega_0^2$ , where the final phonon states exist.

In Fig. 4, the dependences of the line shift and width on the concentration are shown for the point, line, and plain defects. The value of coupling constant  $\lambda = -1$  is taken. We define the full width at half maximum  $\Gamma$  (FWHM) in the usual way:  $\Gamma = \omega_+ - \omega_-$ , where the Raman intensities  $I(\omega_{\pm}) = 0.5I(\omega_{\text{max}})$  and  $\omega_+ > \omega_{\text{max}} > \omega_-$ . The behavior of the width  $\Gamma$  and of the line position  $\omega_{\text{max}}$ , calculated with the help of Eqs. (4), (5), and (6) is shown in the left panel. In the right panel, the Raman line asymmetry  $(\omega_+ - \omega_{\text{max}}) - (\omega_{\text{max}} - \omega_-)$  is plotted. We see that the plain defect affect more intensively on the width and asymmetry, than the line and point defects. To the contrary, the Raman line is shifted more for the point defects.

The cases of the positive coupling constant, when the localized states arise, are shown in Figs. 5 and 6. The accurate results (solid lines) differ considerably from that obtained in the unrenormalized approximation (dashed lines). The maximum that was found in the unrenormalized approximation is smoothed out, transforming into a shoulder with the width of the order of  $\sqrt{c}$  in accord with Eq. (10). Emphasize, that the total number of localized states, integrated over frequency, is proportional to  $c$  independently of the approximation.

The difference in results for defects of different geometries is evident from Figs. 2–6. These distinctions in the Raman line shape and shift can be detected in fitting to the experimental data.

### III. CONCLUSIONS

To summarize, we investigate here the structure of the phonon density of states and the Raman line shape in the situation when localized levels  $\omega_l$  interact strongly with the closely-spaced edge of the extended optical-phonon states. In the linear approximation in defect concentration  $c$ , the contribution of localized states does not have the well-known form of  $\delta$ -function:  $c\delta(\omega - \omega_l)$ , if the effect of defect concentration is more essential than the phonon natural width.

The line shape of bulk-phonon extended states is asymmetrical. The additional width (proportional to the defect concentration) arises on the side of line related to the band of extended states. As a most intriguing example, we would like to compare the behavior of the Raman lines of graphite at  $1600\text{ cm}^{-1}$  and of diamond-like material at  $1300\text{ cm}^{-1}$ . When defects are added to graphite, the low-frequency wing of the line becomes to drop more slowly than the high-frequency wing (see Figs. 1 and 2 in Ref. [13]) in just the same way as shown in Figs. 2 and 3 of the present paper. But if it is diamond samples that are impaired, the opposite, i.e. high-frequency, side slopes more gently (see Fig. 7 in Ref. [13] and Fig. 2 in Ref. [14]). Using the present theory, the explanation of the phenomenon may be attributed to the difference in the phonon dispersion of these substances. Namely, contrary to graphite, there is a minimum of the optical-phonon branch at the Brillouin zone-center in diamond [15].

### IV. ACKNOWLEDGMENTS

The author acknowledges the kind hospitality of Max-Plank-Institute für Physik Komplexer Systeme, Dresden, where this work was performed.

## REFERENCES

- [1] A. Göbel, T. Ruf, J. M. Zhang, R. Lauck, and M. Cordona, Phys. Rev. B **59**, 2749 (1999).
- [2] S. Nakashima, Y. Nakatake, H. Harima, M. Katsuno, and N. Ohtani, Appl. Phys. Letts. **77**, 3612 (2000); see also S. Nakashima, H. Ohta, M. Hangyo, and B. Palosz, Philos. Mag. B **70**, 971 (1994).
- [3] S. Rohmfeld, M. Hundhausen, and L. Ley, Phys. Rev. B **58**, 9858 (1998).
- [4] L. A. Falkovsky, J. M. Bluet, and J. Camassel, Phys. Rev. B **55**, R14 697 (1997); see also **57**, 11 283 (1998).
- [5] S.-I. Tamura, Phys. Rev. B **30**, 849 (1984).
- [6] L. A. Falkovsky, Pis'ma v Zh. Éksp. Teor. Fiz. **66**, 817 (1997) [JETP Lett. **66**, 860 (1997)].
- [7] I. M. Lifshits, Zh. Éksp. Teor. Fiz. **17**, 1017 (1947); I. M. Lifshits, Nuovo Cimento Suppl. **3**, 716 (1956); Usp. Fiz. Nauk **83**, 617, (1964) [Sov. Phys. Usp. **7**, 571 (1965)].
- [8] I. M. Lifshits, S. A. Gredeskul, L. A. Pastur, *Introduction to the theory of disordered systems* (Wiley Interscience, New York, 1988).
- [9] H. Böttger, *Principles of the theory of Lattice Dynamics* (Physik-Verlag, Weinheim, 1983), chap. 2.
- [10] L. A. Falkovsky, Pis'ma v ZETF **71**, 225 (2000) [Sov. Phys. JETP Letters **71**, 155 (2000)].
- [11] A. A. Abrikosov, L. P. Gorkov, and I. E. Dzyaloshinski, *Methods of Quantum Field Theory in Statistical Physics* (Dover, New York, 1963).
- [12] L. A. Falkovsky, Zh. Éksp. Teor. Fiz. **117**, 735 (2000) [JETP **90**, 639 (2000)].
- [13] J. Wagner, M. Ramsteiner, Ch. Wild, and P. Koidl, Phys. Rev. B **40**, 1817 (1989).
- [14] J. W. Ager III, D. K. Veirs, and G. M. Rosenblatt, Phys. Rev. B **43**, 6491 (1991).
- [15] M. Schwoerer-Bohning, A. T. Macrander, and D. A. Arms, Phys. Rev. Lett. **80**, 5572 (1998).

## FIGURES

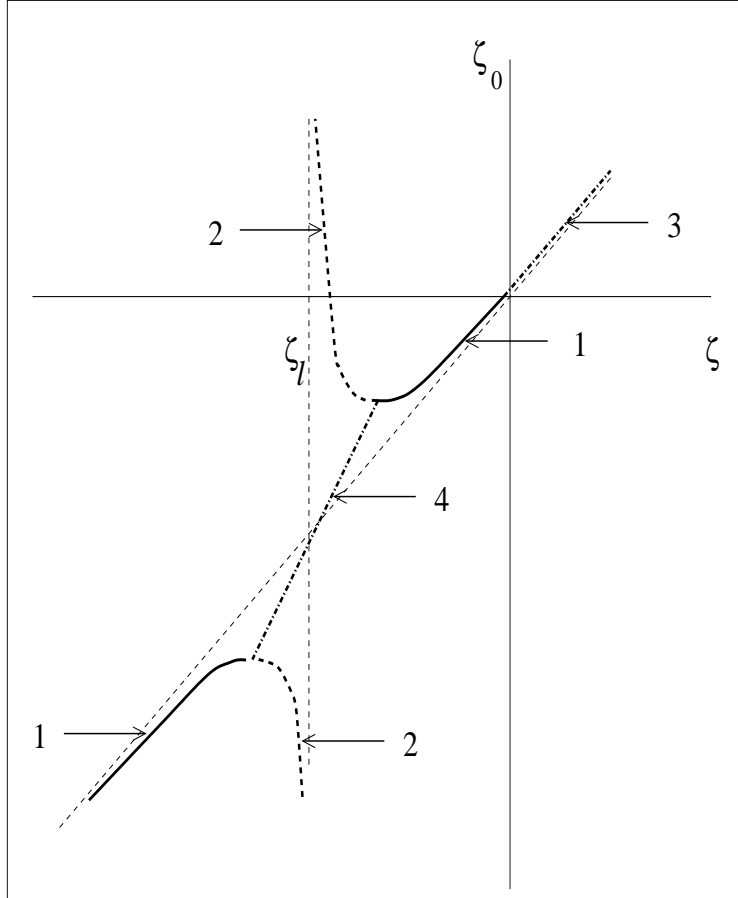


FIG. 1. Plot of function  $\zeta_0(\zeta)$  given by Eqs. (4)–(6). In the regions shown by the dot-dashed lines (indicated by arrows 3 and 4), the solution  $\zeta(\zeta_0)$  has a finite imaginary parts for real  $\zeta_0$ . The region 3 corresponds to the extended phonon mode. The region 4 is related to the localized states.

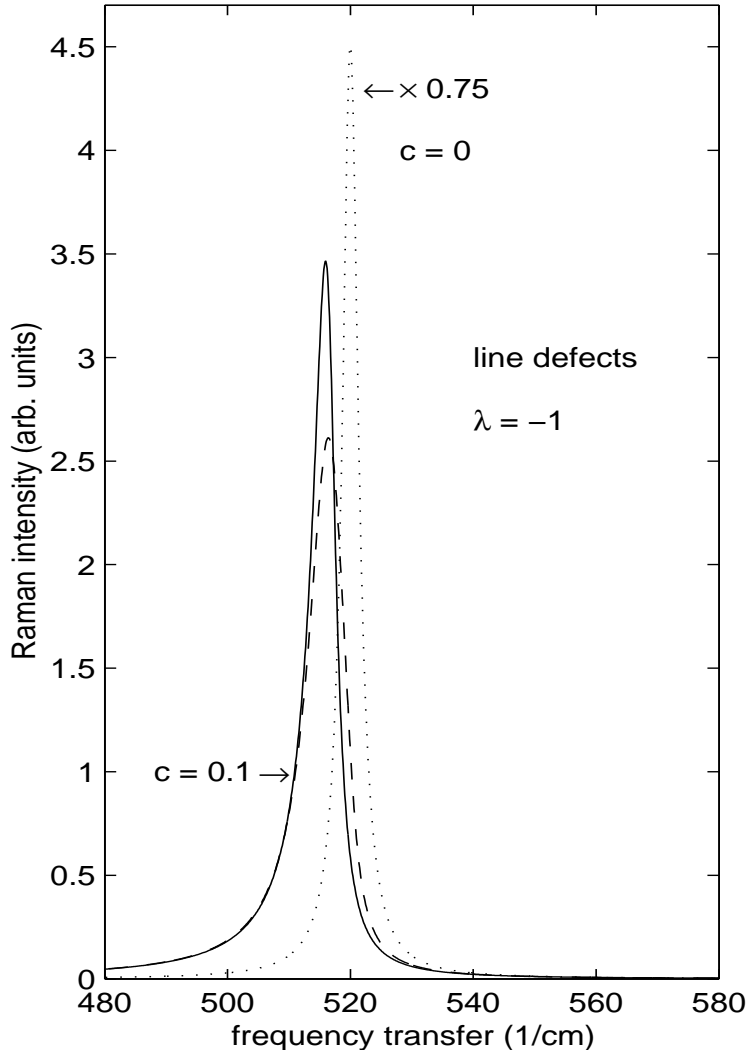


FIG. 2. Imaginary part of the phonon Green's function versus frequency  $\omega$  for parameters of silicon:  $\omega_0 = 520 \text{ cm}^{-1}$ ,  $\Gamma^{\text{nat}} = 3.2 \text{ cm}^{-1}$ . The number of line defect per atomic volume  $c = 0.1$  and the phonon-defect coupling constant  $\lambda = -1$  (the solid line for the self-consistent solution, the dashed line for unrenormalized approximation). The results for pure crystal ( $c = 0$ ) are shown by the dotted line.

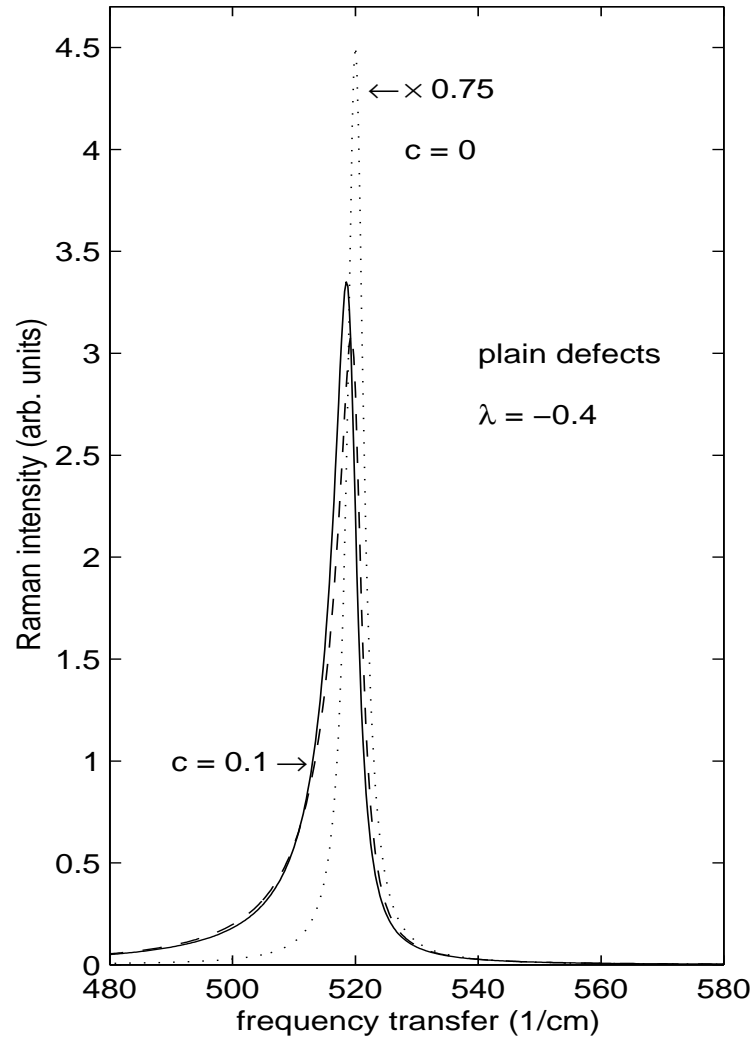


FIG. 3. Same as Fig. 2 but for plain defects with the coupling constant  $\lambda = -0.4$ .

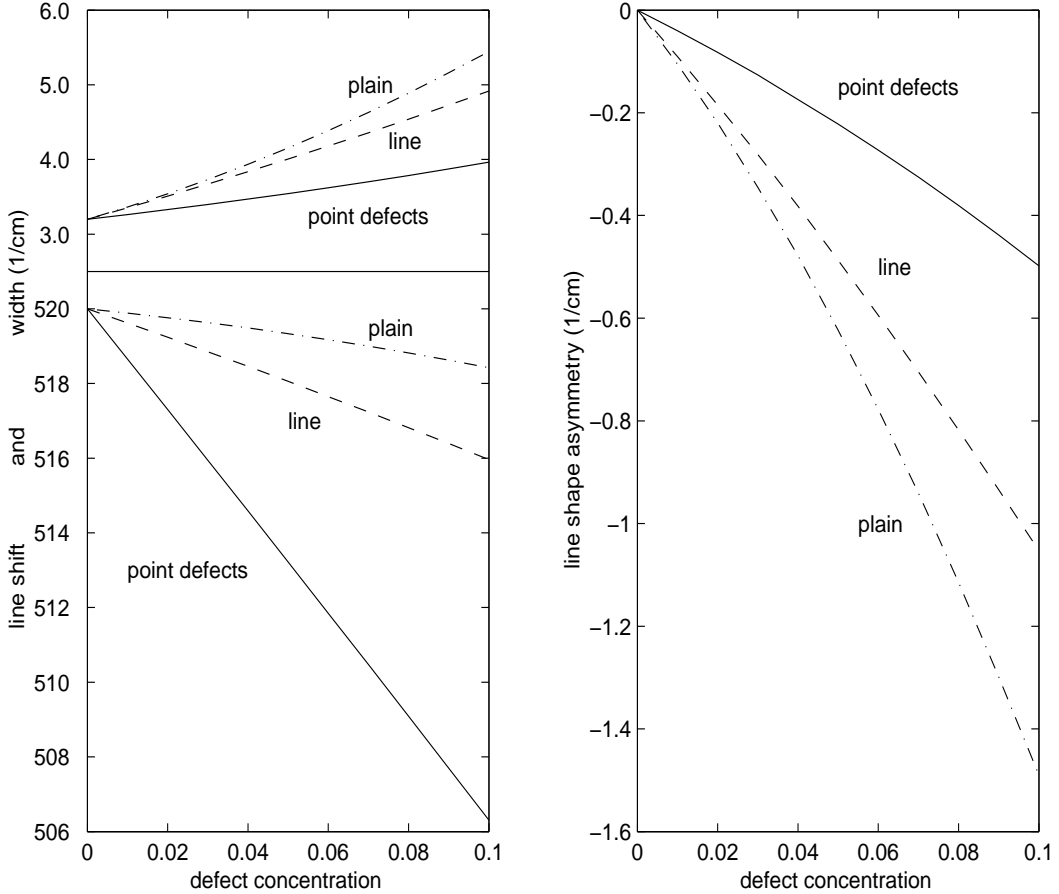


FIG. 4. The theoretical Raman line width (upper part of left panel), shift (bottom part of left panel), and asymmetry (right panel) as functions of the defect concentration. The phonon-defect coupling constant  $\lambda = -1$ . Results for the point, line, and plain defects are plotted by the solid, dashed, and dot-dashed lines, respectively.

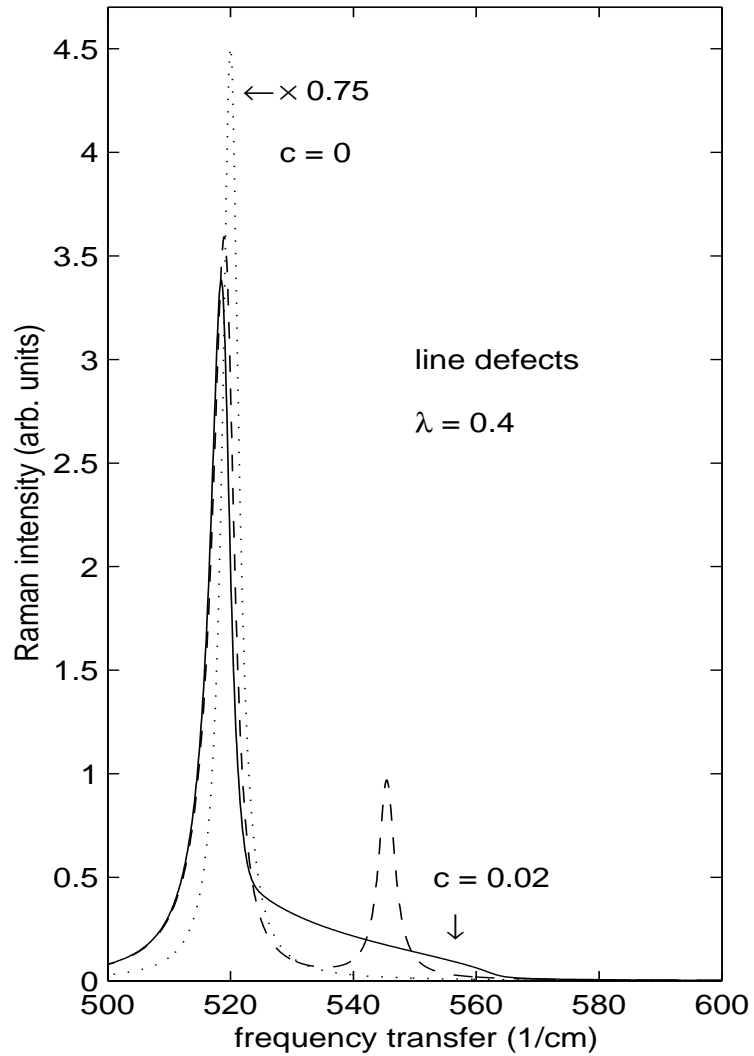


FIG. 5. Same as Fig. 2 but for the positive coupling constant  $\lambda = 0.4$ , when localized states exist. The defect concentration  $c = 0.02$ .

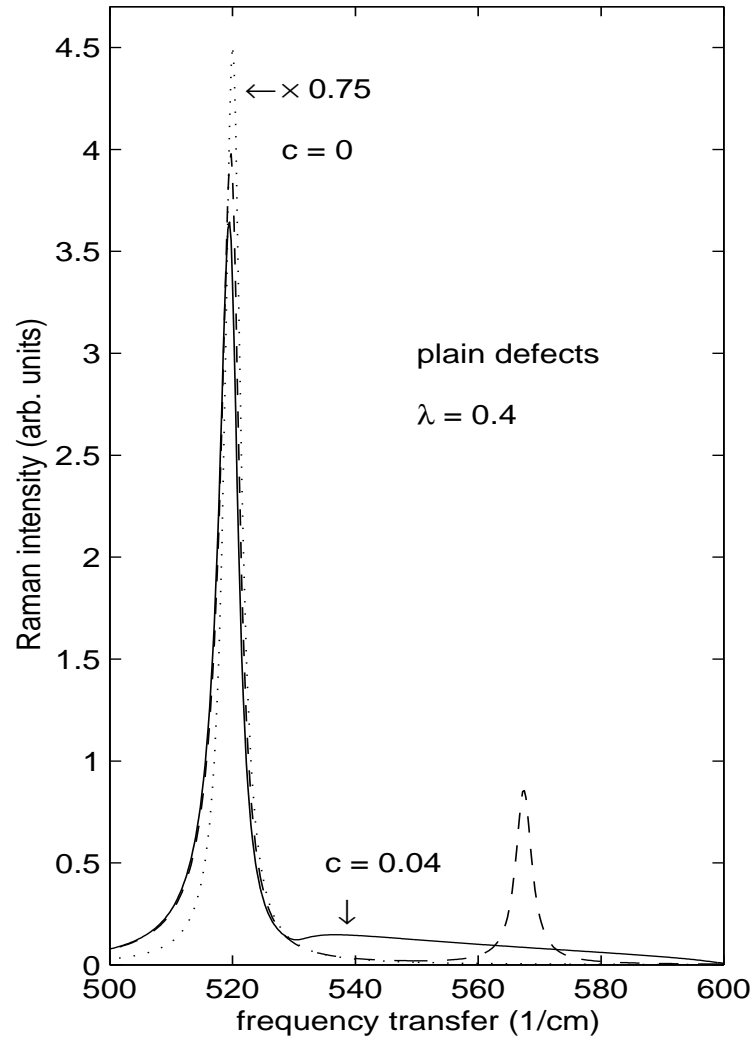


FIG. 6. Same as Fig. 2 but for plain defects with the positive coupling constant  $\lambda = 0.4$  and the concentration  $c = 0.04$ .